Side-Chain Dynamics and Crystallization in a Series of Regiorandom Poly(3-alkylthiophenes)

Shireesh Pankaj, Elke Hempel, and Mario Beiner*

Institut für Physik, Martin-Luther-Universität Halle-Wittenberg, D-06099 Halle, Germany

Received July 19, 2008; Revised Manuscript Received October 8, 2008

ABSTRACT: A series of regiorandom poly(3-alkylthiophenes) [P3ATs] with $4 \leq C \leq 12$ alkyl carbons per side chain are studied by shear, calorimetry, X-ray scattering techniques, and infrared spectroscopy. We show that the tendency of alkyl groups to segregate in small alkyl nanodomains is a common feature of semicrystalline and amorphous members of this series. Semicrystalline poly(3-dodecylthiophene) ($C = 12$) samples show a pronounced lamellar structure with a coherence length of about 150 Å, corresponding to staples of main chain and alkyl nanodomains comparable to the findings for regioregular P3ATs, while the alkyl nanodomains in amorphous P3ATs have more irregular shape and boundaries. An additional relaxation process α_{PE}, which is related to the dynamics of CH_2 units in the alkyl nanodomains, appears in amorphous samples with $C \geq 6$. Its frequency temperature dependence is very similar to that of the α_{PE} process found in other side-chain polymers containing alkyl groups with identical length. This is a strong argument supporting the idea that main chains and alkyl groups separate in amorphous systems. Another interesting finding is the appearance of three distinct melting peaks for regiorandom poly(3-dodecylthiophene) [P3DDT] at temperatures between −10 and 50 °C. Isothermal crystallization experiments are performed, and possible reasons for the appearance of three distinct melting peaks are considered. Similarities and differences between regiorandom and regioregular P3ATs in the semicrystalline state are described and discussed on the basis of their microstructure.

I. Introduction

The relaxation and crystallization behavior of comblike polymers containing long *n*-alkyl groups in the side chain has been extensively studied in the past decades by various groups focusing on different aspects.[1−9] Interestingly, there are dynamic and structural features which seem to be quite common for all these polymers and related to their microstructure. In particular, it has been reported consistently that there is a strong tendency of the individual alkyl groups to aggregate and to form alkyl nanodomains with a typical dimension of about 5−30 Å depending on the length of the alkyl groups.[10,11] This phenomenon, sometimes called nanophase separation,[12,13] is reflected in X-ray scattering data by a "prepeak" at scattering vectors in the range $0.2 \leq q \leq 0.6$ Å^{-1}. Detailed neutron scattering experiments on a series of amorphous poly(*n*-alkyl methacrylates) do strongly support this nanophase separation picture.[14] Higher orders to the prepeak, however, are usually not observed for amorphous samples and only seen in systems with semicrystalline side chains. Thus, the question whether or not the amorphous systems are above or below the order-to-order transition as known from block copolymers is still relevant.[15] A strong argument for nanophase separation in amorphous systems is the appearance of a relaxation process α_{PE}, which occurs in practically all these side-chain polymers[10] at temperatures significantly below the conventional glass temperature T_g, where the polymeric material softens completely on a time scale of minutes. The frequency temperature dependence of the α_{PE} process is basically main chain independent and determined by the length of the alkyl groups, which defines the size of the alkyl nanodomains. It has been shown[10,14,23,24] that the molecular reason for this low-temperature relaxation process are motions within self-assembled alkyl nanodomains. The interpretation is that the alkyl nanodomains preserve their mobility far below the conventional glass transition, where the material behaves macroscopically like a solid. Side-chain mobility does not affect the overall mechanical stability as it is maintained by the rigid skeleton formed by frozen main chains. The features of the dynamics within the alkyl nanodomains change usually from a localized process with an Arrhenius-like temperature dependence for small nanodomains ($d_{nps} < 15$ Å) to a truly non-Arrhenius-like temperature dependence as typical for cooperative relaxation processes in larger domains ($d_{nps} > 15$ Å).[10] This indicates that the dynamics of the CH_2 units is controlled by the size of the self-assembled confinement. Larger deviations from Arrhenius behavior with increasing size can be understood as an indirect hint for an increasing cooperativity of the underlying motions and the existence of dynamic nanoheterogeneities in glass-forming materials.[10,22] In the case of very long alkyl groups a transition from amorphous to semicrystalline alkyl nanodomains will occur. The *C* value where crystallization starts to appear depends on the properties of the main chain, which acts as a constraining element frustrating the side chains and leading to the stabilization of the disordered state in the case of short alkyl groups. Side-chain crystallization starts to occur in many atactic polymers in the range of 8−12 alkyl carbons per side chain. The described behavior has been found qualitatively for various homologous series of side-chain polymers like poly(*n*-alkyl methacrylates),[8,13,25] poly(*n*-alkyl acrylates),[10] poly(*n*-alkyl itaconates),[6,11] and hairy rod polyimides.[26] The features are similar for all these series and in part truly predictable. Potentially, the knowledge about structure−property relationships in such systems could be used to optimize the properties of various materials containing long alkyl sequences.

Prominent examples for side-chain polymers where this knowledge could be applicable are poly(3-alkylthiophenes) (P3ATs, cf. Scheme 1) belonging to the class of conjugated polymers that are environmentally and thermally stable. Polythiophenes are an interesting class of materials due to their favorable electronic, optoelectronic, thermochromic, and solvatochromic properties.[7,27−32] Alkylation helps to improve conductivity, processability, and solubility of thiophene-based materials. Thus, alkyl sequences in the side chain are of major importance for optimizing the properties of such materials. In particular, it is reported that the three-dimensional order and the performance of devices made from such semiconducting

* To whom correspondence should be addressed.

10.1021/ma801633m CCC: $40.75
Published on Web 01/16/2009

Scheme 1

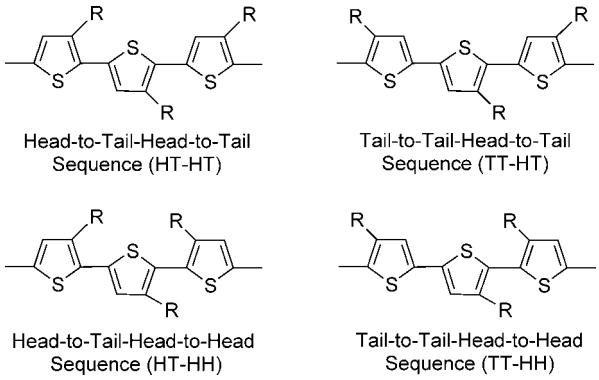

polymers strongly depend on the length of the alkyl groups and their architecture.[33] There are two main classes of poly(3-alkylthiophenes), namely regioregular (100% head−tail−head−tail, HT-HT) and regiorandom samples (random distribution of sequences as shown in Scheme 1). Significant differences in electrical and optical properties of regioregular and regiorandom P3ATs have been reported. Because of their superior properties, which are attributed to high crystallinity and better main-chain packing, regioregular P3ATs are widely used and often studied.[34,35] Calorimetric measurements on regioregular systems show two endothermal peaks. The main peak at high temperatures (between 150 and 250 °C) is commonly related to main-chain melting, and an additional peak occurring around 60 °C has been sometimes interpreted as melting of side-chain crystals.[36,37] The crystalline structure of regioregular thiophenes is also extensively studied.[29,38,39] A lamellar superstructure with main-chain and side-chain-rich regions is reported.[7,40,41] It is also often stated that the packing of regioregular P3ATs is comblike with partly interdigitating alkyl groups. Detailed information about the packing of the side chains is not really available.

We will show in this paper that the features observed in many other series of side-chain polymers with similar microstructure do also appear in a series of regiorandom poly(3-alkylthiophenes) [P3AT] with $4 \leq C \leq 12$ alkyl carbons per side chain. The samples are investigated by shear, calorimetry, and X-ray scattering. The results are compared in detail with findings for a series of atactic poly(*n*-alkyl methacrylates) [PnAMA] with comparable side-chain lengths.[10,13] It is demonstrated that the packing behavior of regiorandom P3ATs as well as their relaxation behavior shows many similarities to that of PnAMAs. The results imply that these systems are suitable to study the interplay between structure, dynamics, and crystallization in small alkyl nanodomains. Peculiarities in the crystallization behavior of regiorandom poly(3-dodecylthiophene) ($C = 12$) indicating polymorphism are observed by calorimetry and studied further by wide-angle X-ray scattering and infrared spectroscopy. The results will be related to questions which are important for a better understanding of dynamics and crystallization of nanostructured polymers as well as typical problems which are relevant for the application of thiophene-based materials.

II. Experimental Section

Samples. A series of regiorandom (1:1:1:1) (HT-HT:HT-HH:TT-HT:TT-HH) poly(3-alkylthiophenes-2,5-diyl) with different number of alkyl carbons per side chain C is studied. Poly(3-butylthiophene) [$C = 4$, P3BT], poly(3-hexylthiophene) [$C = 6$, P3HT], poly(3-octylthiophene) [$C = 8$, P3OT], poly(3-decylthiophene) [$C = 10$, P3DT], and poly(3-dodecylthiophene) [$C = 12$, P3DDT] samples were purchased from Rieke Metals Inc. Important parameters characterizing these polymers are summarized in Table 1. The samples are synthesized using Rieke Zinc in the presence of $Pd(PPh_3)_4$ as catalyst. Further details are described elsewhere.[42]

Table 1. Characteristic Parameters for Regiorandom P3ATs

	no. of alkyl carbons C	T_g/°C (DSC)	T_α/°C (TMDSC)	T_α/°C (DMA)[a]	$T_{\alpha,PE}$/°C (DMA)[a]	d_{nps}/Å
P3BT	4	34	36	45		
P3HT	6	4	9	12	−87	16
P3OT	8	−22	−15	−13	−65	20
P3DT	10		−29	−25	−59	21 (18[b])
P3DDT	12		−31	−18	−49	25 (21[b])

[a] Measurement frequency $\omega = 10$ rad/s. [b] Data for the as-received samples with high degree of crystallinity.

Scattering Experiments. X-ray scattering measurements in the range $0.2\ \text{Å}^{-1} \leq q \leq 0.6\ \text{Å}^{-1}$ were performed on a small-angle instrument assembled by JJ X-rays based on a 2D detector (Bruker HI star) and a Rigaku rotating anode with focusing optics. The measurements were performed at room temperature (22 ± 2 °C) under vacuum using Cu Kα radiation with a wavelength $\lambda = 1.54$ Å. Measurement time was 600 s. The instrument was calibrated using silver behenate as reference material. The samples were pressed significantly above T_g and melting temperature T_m under a hot press for 5 min. In the case of P3DDT and P3DT as-received samples with comparably high crystallinity were measured for comparison. Additional wide-angle X-ray scattering measurements on P3DDT samples are performed using a SIEMENS D5000 powder diffractometer with germanium monochromator.

Dynamic Mechanical Analysis. The dynamic shear modulus $G^* = G' + iG''$ was measured in the frequency range from 0.1 to 100 rad/s with a control strain of 0.1% using a Rheometrics RDAII instrument. The experiments were performed on small sheets with dimensions of about $10 \times 10 \times 1\ \text{mm}^3$. All samples were pressed in the viscous state to stripes using a hot press and then mounted immediately in the rheometer at room temperature. Measurements are performed between −120 and 40 °C with a step of +3 K. Samples were annealed for 60 s at each temperature prior to the frequency sweep. All the measurements were done under a controlled nitrogen gas atmosphere.

Thermal Analysis. A Perkin-Elmer DSC 7 was used (i) for cooling and heating scans with rates of $dT/dt = \pm 20$ K/min and (ii) for temperature-modulated DSC (TMDSC) measurements performed with sawtooth modulation (time period $t_p = 60$ s, underlying scan rate $dT/dt = 4$ K/min). Samples with a mass of about 10 mg were used and encapsulated in closed DSC pans under a controlled nitrogen atmosphere.

Infrared Spectroscopy. Vibrational spectroscopy experiments on P3DDT films with a thickness of about 100 μm are performed using a Bruker TENSOR 37 FT-IR spectrometer.

III. Results

X-ray scattering data for the investigated series of regiorandom P3ATs are shown in Figure 1a. A prepeak in the range $0.2\ \text{Å}^{-1} \leq q \leq 0.6\ \text{Å}^{-1}$ is observed for all samples, indicating the existence of a characteristic length scale in the 1 nm range. The prepeak sharpens slightly and shifts systematically to the lower scattering vectors q with increasing number of methylene units in the alkyl side chains. The maximum of the prepeak for P3HT ($C = 6$) is observed at approximately $q_{max} = 0.39\ \text{Å}^{-1}$ while it appears at $q_{max} = 0.255\ \text{Å}^{-1}$ for P3DDT ($C = 12$) in the amorphous state. According to Bragg's law $d = 2\pi/q_{max}$ this corresponds to equivalent Bragg spacings d_{nps} in the range 16−24.5 Å. For as-received P3DT and P3DDT samples ($C = 10, 12$), the prepeak looks significantly sharper, indicating a better long-range order of the corresponding structure. This behavior is well-known from other semicrystalline side-chain polymers where the CH_2 units in the alkyl nanodomains are able to crystallize like higher poly(*n*-alkyl methacrylates) with $C \geq 12$ methylene units.[43] Coherence lengths d_S as estimated using the Scherrer equation are about 85 Å for amorphous samples and about 150 Å for as-received, semicrystalline

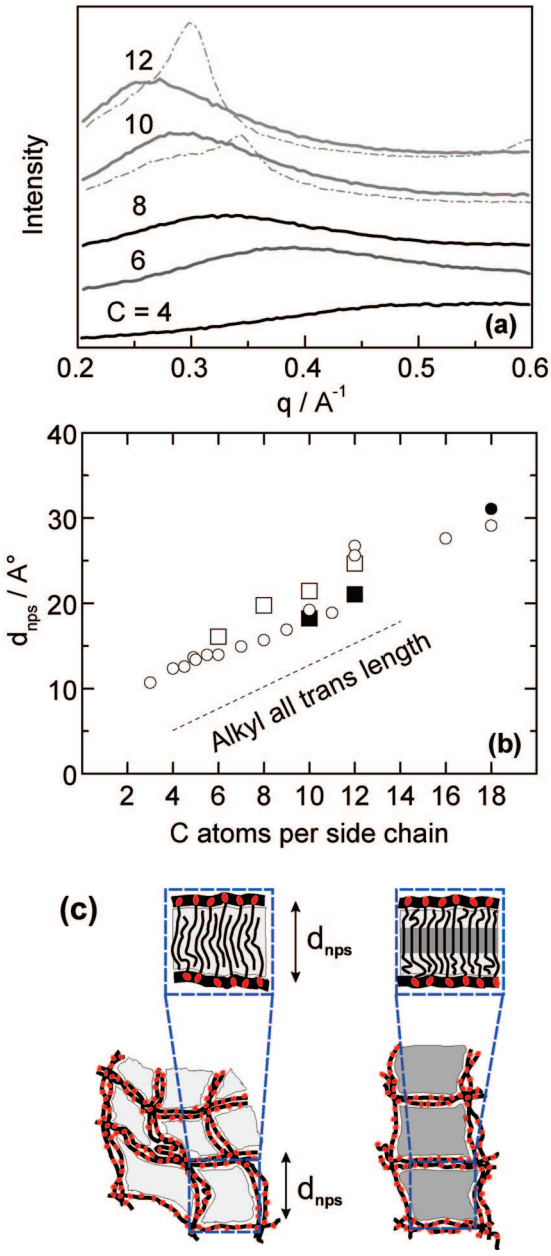

Figure 1. (a) Intensity vs scattering vector q for a series of regiorandom P3ATs (solid lines). The labels indicate the number of alkyl carbons per side chain C. Results for as-received, semicrystalline P3DT ($C = 10$) and P3DDT ($C = 12$) samples (dashed-dotted lines) are shown for comparison. All measurements are performed at room temperature. (b) Equivalent Bragg spacings $d_{nps} = 2\pi/q_{max}$ as obtained from the prepeak positions in (a) as plotted versus number of carbon atoms per side chain C (squares). Hollow symbols denote amorphous and solid squares denote crystalline samples. Data for a series of atactic poly(n-alkyl methacrylates) (small circles[10]) are given for comparison. The thin line indicates the slope, which is expected for extended (all trans) alkyl groups. (c) Schematic pictures showing the structure of nanophase-separated side-chain polymers in the amorphous (left) and semicrystalline (right) state. The situation in a single alkyl nanodomain is sketched in the upper parts while a more global view is given in the lower parts. Amorphous methylene sequences are indicated by light gray and crystalline parts by dark gray.

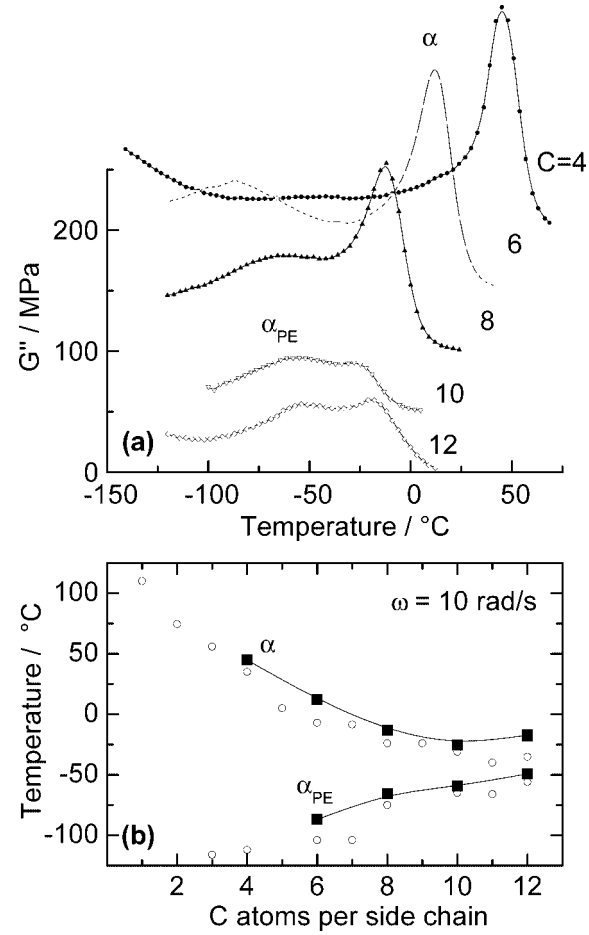

Figure 2. (a) Shear loss modulus G'' vs temperature for regiorandom P3ATs measured at a frequency of 10 rad/s. The measurements are performed in heating with an average rate of about +2K/min. The curves are vertically shifted (50 MPa/curve) for reasons of clarity. (b) Relaxation temperatures vs C number for regiorandom P3ATs (full squares). Peak maxima are taken from isochronal shear curves $G''(T)$ measured at 10 rad/s by fitting the data using Gaussian functions. Data for previously measured PnAMA are shown for comparison (open circles[13]).

P3DDT.[44] The appearance of higher orders to the prepeak in semicrystalline samples like P3DDT shows that a lamellar structure corresponding to staples of main chains and alkyl nanodomains exists in these samples (Figure 1c). A straightforward explanation for the occurrence of a prepeak in the amorphous members is a strong tendency of the alkyl chains belonging to different monomeric units to aggregate and to form alkyl nanodomains. Demixing effects leading to the formation of alkyl nanodomains with more irregular shape and boundaries seem to occur already in the amorphous state.[15] The average main chain to main chain distances d_{nps} for P3ATs and previously studied PnAMAs[10,13] are comparable, as shown in Figure 1b. In particular, the increase of d_{nps} with C is similar for both series. If compared with the all-trans length of the alkyl chains, a nearly uniform offset seems to exist for all amorphous members. This finding is consistent with structural models assuming interdigitated side chains and main-chain domains, which are responsible for the constant offset in Figure 1b. Comparing the data for semicrystalline P3DT ($C = 10$) and P3DDT ($C = 12$) with their amorphous counterparts, one can conclude that d_{nps} decreases slightly during crystallization. This behavior corresponds to the expected densification of the system during crystallization but is in contrast to the observation for crystallizable PnAMAs where an opposite trend has been reported and interpreted as a consequence of an increasing trans content in the alkyl groups.[43,45] This may indicate differences in the packing and will be discussed in some detail below.

Dynamic mechanical measurements on our P3ATs series show a clear dependence of the relaxation behavior on the side-chain length (Figure 2a). The α relaxation process in shear loss modulus "G" curves moves to lower and lower temperatures (Figure 2b) with increasing number of CH_2 groups in the side

chains. The α peak appears at about 45 °C for P3BT ($C = 4$) and approaches −18 °C for nearly amorphous P3DDT ($C = 12$). The relaxation temperature as obtained from Gaussian fits to "G"(T) isochrones measured at 10 rad/s saturates for higher members of regiorandom P3ATs. A similar shift of α relaxation process and DSC glass temperature T_g has been reported for atactic PnAMAs. The relevant data are shown for comparison in Figure 2b. The shift of the α relaxation process in the PnAMA series has been related by Heijboer in the 1960s[46] to an "internal plasticization" of the main chains by the highly mobile alkyl groups in the environment. The most interesting feature in the shear curves for regiorandom P3ATs with $C \geq 6$ is that an additional relaxation process (α_{PE}) appears at temperatures below the conventional α relaxation. This process occurs in the same temperature frequency range where the "polyethylene-like glass transition" α_{PE} has been reported for PnAMAs and other polymer series with long alkyl groups in the side chain.[10] The α_{PE} process shifts systematically to higher temperatures with increasing number of methylene units per side chain and becomes stronger compared to the intensity of the conventional α relaxation peak. In the case of atactic PnAMAs it has been shown that the α_{PE} process in members with $C \geq 8$ is related to cooperative motions of the CH_2 units in small alkyl nanodomains. Thus, this relaxation process has been interpreted as a "polyethylene-like glass transition" α_{PE}. For PnAMAs with $4 \leq C < 8$, the α_{PE} process seems to be more a Johari−Goldstein-like[47] secondary relaxation β_{PE} with Arrhenius-like temperature dependence incorporating CH_2 units in the alkyl nanodomains.[22] The appearance of similar relaxation processes in amorphous, regiorandom P3ATs fits to the recent observation that the frequency temperature position of the α_{PE} process in nanophase-separated side chain polymers is practically independent of microstructure and softening behavior of the main chains.[10] The values for the steepness index $m = -\mathrm{d}\log\omega/\mathrm{d}(T_{\alpha,10\mathrm{rad/s}}/T)|_{T=T_{\alpha,10\mathrm{rad/s}}}$ show a significant scatter in the range $m \approx 25$ for $C = 6-12$, which is in qualitative agreement with previous findings for other side-chain polymers. Hence, the reported shear data for P3ATs support the idea that the tendency of main- and side-chain parts to separate is a general phenomenon in comblike polymers containing long alkyl groups. Note that there is no clear evidence for an α_{PE} process in P3BT. In light of this fact and the occurrence of a broad prepeak in the scattering data for P3BT (Figure 1a), it seems to be open whether or not P3ATs with very short alkyl groups are really nanophase separated. An additional, tiny β process is indicated in the shear curve for P3BT ($C = 4$) at about −45 °C, which is not seen for all higher P3ATs (Figure 2a). It is hard to get further information about the existence of this process in the higher members based on relaxation spectroscopy data since strong contributions related to α and α_{PE} occur in the same frequency temperature range. One may speculate that the β process is hidden due to an overlap with the two prominent relaxation processes (α and α_{PE}) in these samples.

DSC heating scans for regiorandom P3ATs, performed after removing the thermal history of as-received samples by annealing at 150 °C for 5 min, show that a thermal glass transition occurs for all samples indicated by a prominent step in $c_p(T)$ (Figure 3a). As expected, the glass temperature T_g, obtained from an equal area construction (inset of Figure 3a), decreases with increasing side-chain length C. The T_g shift is 10−15 K per additional CH_2 unit in the side chain (Table 1). For P3DDT with $C = 12$ alkyl carbons per side chain, the glass temperature is hard to estimate based on the heating scans since additional contributions occur slightly above T_g. There are two small peaks in $c_p(T)$ for this sample. TMDSC measurements are performed in order to clarify the nature of these peaks. TMDSC results presented in Figure 3b show real and imaginary parts of the

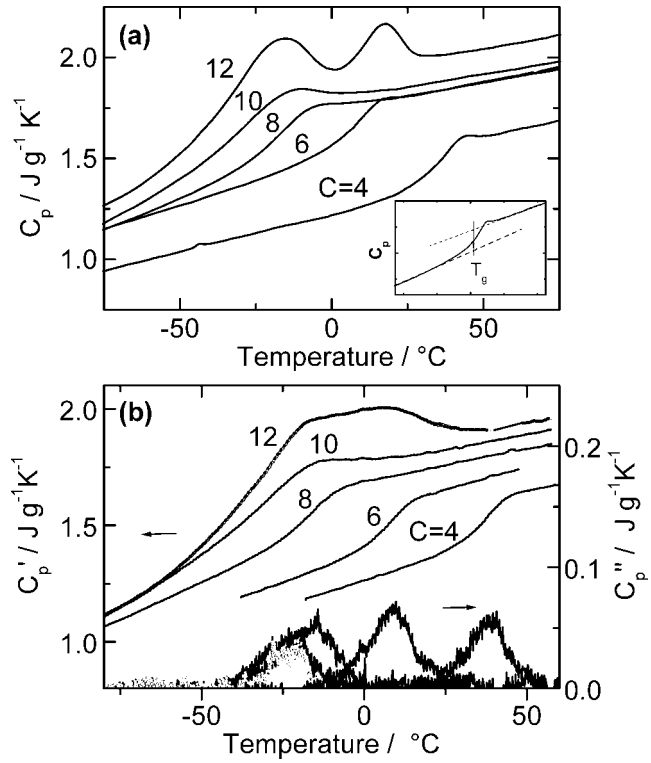

Figure 3. (a) DSC heating scans ($\mathrm{d}T/\mathrm{d}t = +20$ K/min) and (b) TMDSC data ($t_p = 60$ s) for a series of regiorandom P3ATs. The labels indicate the C number. The inset in (a) shows the method to calculate T_g using an equal area construction.

dynamic heat capacity $c_p^*(T) = c_p' - ic_p$. Dynamic glass temperatures T_α (Table 1) are determined by fitting the peaks in the imaginary part, which indicate the α relaxation process, using a Gaussian function. Additional features following the glass step are seen in the real parts c_p' for P3DT ($C = 10$) and P3DDT ($C = 12$). This shows that the peaks in the DSC scans are not simply overshoots resulting from nonequilibrium effects in glass-forming materials. Interestingly, the results seem to indicate that there are two weak melting peaks in P3DDT including reversible contributions detectable by TMDSC. This phenomenon is studied further below.

DSC heating scans for differently prepared P3DDT ($C = 12$) samples are presented in Figure 4a. A relatively large melting peak (I) at 44.5 °C is seen for the as-received sample, while a two-peak feature (II and III) is observed for DSC scans performed after slow cooling (−20 K/min). Peak III has an onset at about −25 °C, and peak II starts at about 5 °C. The large melting peak I at 44.5 °C, which was seen for the as-received sample, is not observed in this case. The double-peak feature was retraceable after fast quenching from 80 to −60 °C with a nominal rate of −200 K/min. This indicates that even fast quenching cannot avoid crystallization during cooling indicated by these two weak melting peaks. In order to clarify further details, isothermal crystallization experiments at different temperatures ($T_c = -25$, 5, and 26 °C) have been performed. This corresponds to temperatures near the onset of the melting peaks III, II, and I as seen in Figure 4a. The crystallization time t_c was varied between 5 min and 7 h at each temperature T_c. The results of isothermal crystallization experiments are presented in Figure 4b. Heating scans measured after crystallization at $T_c = -25$ °C show an increase of peak intensity and a shift of the peak position with time t_c. The results indicate that heat of fusion ΔH_{III} as well as melting temperature $T_{m,III}$ do systematically increase. A weak additional peak (II) at about 20 °C is seen in all scans. This peak remains practically unaffected if t_c is varied.

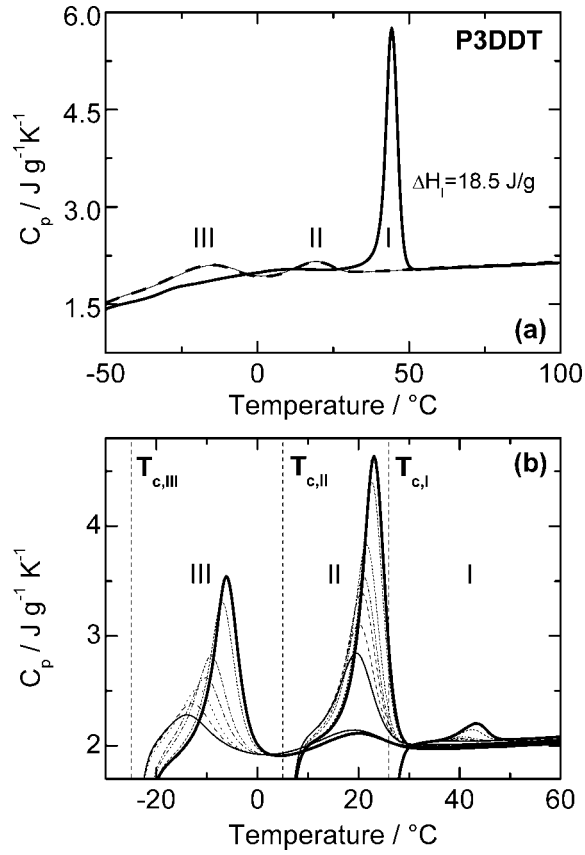

Figure 4. Results from crystallization experiments on regiorandom P3DDT ($C = 12$). (a) DSC heating scans ($dT/dt = 20$ K/min) performed on samples with different thermal history. Scans for the as-received sample (thick solid line), a second scan after slow cooling to −60 °C with $dT/dt = -20$ K/min (thin solid line), and a third scan after quenching to −60 °C with $dT/dt = -200$ K/min (thick dashed line) are compared. (b) DSC heating scans ($dT/dt = 20$ K/min) preformed after isothermal crystallization for different times t_c (from bottom to top: 5, 10, 20, 30, 60, 240, 420 min) at $T_c = -25$, 5, and 26 °C. The labels I, II, and III indicate the different melting peaks.

The crystalline fraction related to this peak is probably formed during cooling from 80 to −60 °C. Results from isothermal crystallization experiments at $T_c = 5$ and 26 °C show that similar changes with time t_c are observed for peak II and peak I, respectively. Additional contributions at other temperatures are not observed under these conditions. The dependence of the heats the fusion ΔH_I, ΔH_{II}, and ΔH_{III} on isothermal crystallization time t_c measured at different temperatures T_c is compared in Figure 5. Obviously, the degree of crystallinity D_c increases in all cases on logarithmic time scales. Clear indications for a significant primary crystallization step are not observed. The melting temperatures T_m of the crystals grown at different temperatures T_c are obviously not comparable; i.e., the crystalline state seems to depend significantly on the crystallization conditions. In general, melting seems to appear in the same temperature range like in case of alkanes and other side-chain polymers containing crystallizable alkyl groups with similar length.[43,48] Note that the occurrence of alkyl groups, which can crystallize either on a hexagonal or an orthorhobic lattice, has been reported recently for eicosylated poly(ethylenimine) with $C = 20$ alkyl carbons in the side chain.[49,50] A resulting question is whether the appearance of different T_m values depending on the crystallization conditions indicates polymorphism in P3DDT, i.e., the existence of different crystalline forms, or it is a result of other effects like differences in crystal size.

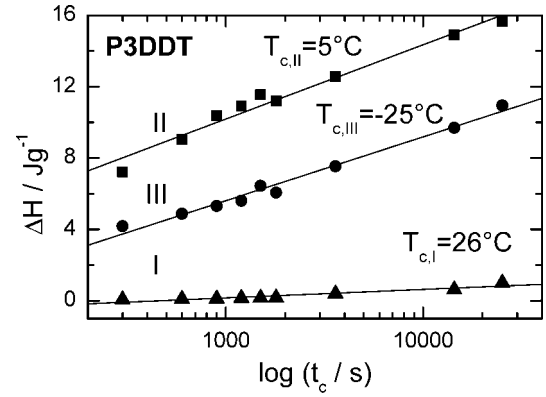

Figure 5. Heat of fusion ΔH vs crystallization time t_c for regiorandom P3DDT measured at $T_c = -25$, 5, and 26 °C. Heats of fusion are calculated based on the area of the melting peaks as shown in Figure 4b.

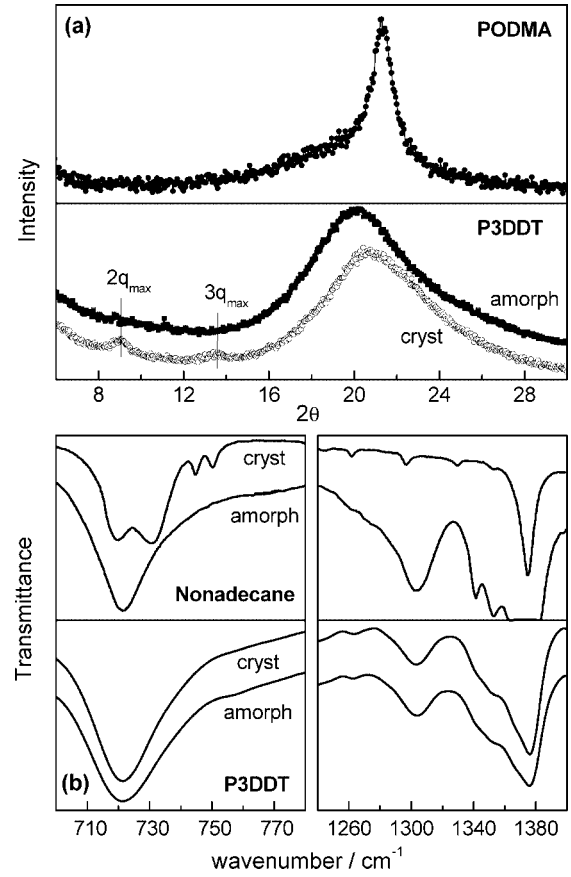

Figure 6. (a) Wide-angle X-ray scattering and (b) infrared spectroscopy data for regiorandom P3DDT measured at room temperature. WAXS data for a semicrystalline sample (open circles) and a practically amorphous P3DDT sample produced by fast melt quenching with −200 K/min (full squares) are compared. Higher order peaks belonging to the prepeak at $2q_{max}$ and $3q_{max}$ are labeled. Results for poly(*n*-octadecyl methacrylate) in the semicrystalline state (full circles) from ref 43 are shown for comparison. IR spectroscopy data for the as-received, semicrystalline (cryst), and the quasi-amorphous quenched (amorph) P3DDT sample are presented. IR results for nonadecene in the molten state (amorph, 29 °C) and in the orthorhombically packed crystalline state (cryst, 19.5 °C) taken from ref 54 are shown for comparison.

A standard methodology to answer this question is to perform wide-angle X-ray scattering (WAXS) measurements. The results of such experiments on differently prepared P3DDT samples are presented in Figure 6a. Obviously, the WAXS data do not show a clear difference between the as-received sample, which should have according to our DSC data a relatively large degree

of crystallinity D_c, and a freshly quenched sample containing presumably only a very small fraction of crystalline material. The main feature in all WAXS curves is an intense amorphous halo at $2\Theta = 20°-21°$ corresponding to $q = 4\pi \sin(\Theta)/\lambda = 1.41-1.49$ Å^{-1}. The shape of this halo is not significantly affected by the chosen program. The only difference might be a weak shoulder in the range $22° \leq 2\Theta \leq 23°$ ($1.56 \leq q \leq 1.63$ Å^{-1}). It is well-known that WAXS pattern of side-chain polymers containing a significant fraction of hexagonally packed methylene units in the alkyl groups are characterized by a sharp peak at $2\Theta \approx 21°$ ($q \approx 1.49$ Å^{-1}) as seen in the poly(*n*-octadecyl methacrylate) [PODMA] data in Figure 6a.[43,45,51] In the case of orthorhomically packed methylene units a second peak should appear at around $2\Theta = 23.5°$ ($q = 1.66$ Å^{-1}).[49] Obviously, clear peaks related to the crystalline fraction are not seen in WAXS data for our P3DDT sample. The shoulder at $22° \leq 2\Theta \leq 23°$ indicates a small crystalline fraction. Information about the packing of the crystalline methylene units, however, cannot be extracted from WAXS data for regiorandom P3DDT. The problem is that the relevant scattering peaks sit on top of a strong amorphous halo since the degree of crystallinity is very small as compared to those of other semicrystalline side-chain polymers studied in the literature. One can estimate based on existing information about the heat of melting for different crystalline forms ($\Delta h_{hex} = 3.07-3.4$ kJ/mol,[48,50] $\Delta h_{ortho} = 3.4-3.99$ kJ/mol,[48,52] $\Delta h_{triclin} = 4.2$ kJ/mol[50]) that at most 9% of the CH_2 units are crystalline. Note that the WAXS data for semicrystalline PODMA shown for comparison in Figure 6a are measured on a sample containing ≈30% crystalline CH_2 units.[43,49] The presented results demonstrate that DSC is a very sensitive tool to detect small fractions of crystalline material that are not easily detectable by WAXS experiments.

Further attempts to verify structural changes and differences in the crystalline packing of the methylene sequences have been made by infrared spectroscopy. This method has been often used to learn more about the crystalline state of alkanes,[53,54] polyethylene,[55] and long CH_2 sequences in side-chain polymers.[49] IR data for P3DDT in the spectral ranges around 720 cm^{-1}, where CH_2 rocking modes have been reported for crystalline methylene sequences,[53,55] and near 1375 cm^{-1}, where usually a CH_3 group deformation (U mode) and CH_2 wagging modes do appear,[53] are shown in Figure 6b. Results for the as-received P3DDT sample having the highest accessible degree of crystallinity (cf. Figure 4a) are compared with that for a freshly quenched sample, which is practically amorphous. The results show that there are no significant differences between both samples. IR spectra of P3DDT in both states are quite similar to that for molten nonodecane in this wavenumber range (Figure 6b) and quite different from that for orthorhombic nonadecane crystals.[53] Effects that allow to analyze the structure of semicrystalline P3DDT like a series of additional bands below 720 cm^{-1} related to CH_2 rocking modes reported for crystalline methylene sequences[49,53,54] are not observed. There is also no detectable shift of the CH_3 band near 1375 cm^{-1} and no clear indication for the disappearance of higher CH_2 wagging modes below 1375 cm^{-1} being additional features reported for crystalline alkyl groups.[53]Presumably, this is again a consequence of the small degree of crystallinity of the investigated P3DDT sample. The presented results show clearly that it is hard to get detailed information about the structure of regiorandom P3DDT in the crystalline state based on standard techniques like X-ray scattering and vibration spectroscopy. More sophisticated methods like NMR[25] should be applied in the future to clarify structural questions related to the packing of CH_2 sequences in higher P3ATs.

IV. Discussion

Summarizing the experimental results for the investigated series of regiorandom poly(3-alkylthiophenes), one can conclude that the experimental findings support physical pictures considering a strong nanophase separation tendency of main chains and alkyl groups as derived from the results for other series of side-chain polymers.[10,14] In accordance with this picture, a prepeak occurs in the X-ray scattering data for all studied P3ATs that shifts systematically to smaller q values, if the number of CH_2 units per side chain increases. According to the oversimplified structural model shown in Figure 1c, this indicates average main chain to main chain distances d_{nps} between 16 Å for P3HT and 24.5 Å for P3DDT. On the basis of the average increase Δd_{nps} of about 1.4 Å per CH_2 unit and a comparison with the length of fully crystalline CH_2 sequences in alkanes (Figure 1b), one may conclude that the disordered alkyl groups are interdigitated and not too far from an extended conformation. The relatively large width of the prepeak in the scattering pattern and the absence of related higher orders in all amorphous samples shows, however, that the underlying nanostructure is far away from being perfect. The estimated coherence length d_S is small (≈65−85 Å[44]), and the structure is in no case a simple arrangement of perfect lamellar stacks. Nevertheless, the tendency of the methylene sequences to form alkyl nanodomains is strong and the overall situation in the system is characterized by a pronounced periodicity in the 1 nm range. Although some points still need further investigation,[15] such a nanophase separation picture seems to be the most natural explanation for the existence of an independent dynamics in the alkyl nanodomains (α_{PE}) comparable to that in other side-chain polymers with a similar microstructure. Thus, the schematic pictures in Figure 1c might be understood as a suitable zeroth approximation to describe the structure of amorphous regiorandom P3ATs. Similar approaches to describe the structure have been reported for other side-chain polymers.[10,11,14] Interestingly, one can understand and predict special properties of these polymeric systems, like special features in their dynamics, already based on such a simplified picture.

That structure−property relationships do really exist can be concluded from the observation that regiorandom P3ATs with $6 \leq C \leq 12$ show an additional relaxation process α_{PE} appearing practically at the same temperature like in other side-chain polymers with identical length of the alkyl group. The α_{PE} process is always found significantly below the conventional α relaxation, i.e., mainly at temperatures where the system is in the glassy state and the main chains are frozen. One can interpret the α_{PE} process as a relaxation process occurring within the alkyl nanodomains and reflecting the (more or less cooperative) motions of many CH_2 units. Such a relaxation process incorporating only the methylene sequences is still possible although the main chains are immobile and the polymer behaves macroscopically like a glass. There is also no conflict in considering two cooperative processes since they occur at different length scales. The α_{PE} process is restricted to the alkyl nanodomains while the α process requires cooperative motions of complete monomeric units. It is important to mention again that typical features characterizing dynamic glass transitions have been found for the α_{PE} process in atactic poly(*n*-alkyl methacrylates), poly(*n*-alkyl acrylates), and poly(*n*-alkyl itaconates) with $C > 8$ alkyl carbons. The non-Arrhenius-like temperature dependence of the relaxation time and a calorimetric activity of the α_{PE} process have been reported.[10] It is hard to prove directly whether or not similar features exist in regiorandom P3ATs. Values for the steepness index $m > 16$ indicate non-Arrhenius behavior, although the uncertainties are still large either due to the small volume fraction of alkyl groups ($C \leq 8$) or due to their crystallization ($C \geq 10$). Crystallization may also explain why significant calorimetric signals for the α_{PE} process cannot be detected in the investigated P3ATs. Alternatively, this might be due to the fact that all noncrystallizable

alkyl groups are too short to show significantly cooperative motions of the CH_2 units. Possibly, the temperature dependence of the α_{PE} relaxation is still close to the Arrhenius limit, and one should talk about a β_{PE} process in amorphous P3ATs. The appearance of side-chain crystallization in regiorandom P3ATs with relatively short side chains ($C \approx 10$) might be related to specialties in the microstructure of P3ATs as discussed below.

Another interesting finding is the existence of three distinct melting temperatures for P3DDT ($C = 12$) depending on the crystallization conditions. The results indicate that the crystallization mechanism is strongly influenced by the crystallization temperature (Figure 4b). The similarity of melting and crystallization temperatures to those reported for alkanes[48,56] and side-chain polymers containing alkyl groups with comparable length[43,49] implies that side-chain crystallization occurs. A crystallization mechanism incorporating main chains like in regioregular P3ATs seems to be unlikely since the melting temperatures in these cases are usually much higher (150 °C $\leq T_m \leq$ 250 °C).[38] A direct proof showing that side-chain crystallization occurs is still under investigation. Apart from the T_m argument, the proposed side-chain crystallization picture is supported by indirect arguments coming from X-ray scattering measurements in the range 0.2 Å$^{-1} \leq g \leq$ 0.6 Å^{-1}. These experiments show clearly that regiorandom P3DDT behaves like other polymers undergoing side-chain crystallization. In particular, a regular order of lamellar stacks with a Bragg spacing of about 21 Å is found in semicrystalline P3DDT (Figures 1a and 6a). The reasons for the appearance of three distinct melting peaks are much more unclear. A straightforward interpretation is to assume that different crystalline forms can occur. It would be very interesting if methylene sequences in the hexagonal, orthorhomic, and triclinic form (known from different alkanes[48,56]) would appear for regiorandom P3DDT. A transition from hexagonal to orthorhombic packed alkyl groups has been reported so far only for very long side chains containing more than 18 alkyl carbons.[49] The observed differences in T_m might be of the right order of magnitude, but structural evidence is not yet accessible. Standard methods are not sensitive enough to give useful information about the crystalline lattice in a system with an extremely small degree of crystallinity ($D_c < 10\%$ of the CH_2 units). An alternative interpretation based on different crystal sizes seems not really reasonable, since one has to explain then why three distinct crystal thicknesses appear, which can even coexist under certain conditions. A common observation for all investigated crystallization conditions is that the melting temperature increases slightly but systematically with increasing heat of fusion ΔH (Figure 4b). Similar behavior has been found for the secondary crystallization in many other side-chain polymers containing long alkyl sequences (e.g., poly(*n*-octadecyl methacrylate[43]) and attributed to crystal thickening since the Gibbs−Thomson equation predicts $\Delta T_m \propto d^{-1}$. In most of these cases, a pronouced step in the D_c vs log t_c curves appears which has been interpreted as primary crystallization step. This step is practically absent in the data for P3DDT shown in Figure 5. A possible scenario to explain this behavior might be to assume that (i) an extremly thin crystalline layer is growing laterally in the alkyl nanodomains of regiorandom P3DDT and that (ii) this crystalline layer starts immeadiately to thicken. The ratio of the time constants for both processes determines then the curve shape in a D_c vs log t_c plot. Other scenarios assuming that only a very few sequences along the main chain are able to crystallize in a similar fashion like in regioregular P3ATs seem to be unlikely since the melting temperatures are too different from that in regioregular P3ATs. Moreover, it is not understandable in this picture why the ability of regiorandom P3ATs to crystallize increases systematically with increasing side-chain length.

Finally, we will consider whether or not the findings for regiorandom P3DDT can contribute to a better understanding of the crystallization in regioregular P3ATs. The main observation is that the overall arrangements of main chains and side chains in systems with regioregular and regiorandom microstructure are similar. In both types of systems, a lamellar pattern in the scattering data occurs, indicating that main-chain and side-chain-rich regions are arranged in stacks. The only difference is the Bragg spacing which is a somewhat smaller in case of regiorandom P3ATs compared to their regioregular counterparts ($d_{nps} = 21$ Å for crystalline, regiorandom P3DDT vs $d_{nps} = 26.2$ Å for regioregular P3DDT[38]). This might be a consequence of differences in the packing of the side chains. While our results for regiorandom P3DDT are consistent with intercalated and nearly extended alkyl groups, the spacings observed for regioregular P3ATs are significantly larger and do not fit to such a picture. This might be understood as an argument for the idea that the alkyl groups are "partly intercalated" and slightly tilted.[29,33] A questionable point of this model seems to be the existence of energetically unfavorable voids. From a general point of view, the main difference between regioregular and regiorandom P3ATs might be that the main chains can pack on one and the same crystalline lattice in the case of regioregular samples, while this is impossible in regiorandom systems since the monomeric units are attached to the main chain randomly with head or tail. The specialty of regioregular P3ATs compared to many other side-chain polymers with similar microstructure could be the fact that the internal distances, including the very regular distance between two side chains along the main chain, fit quite well to ordinary lattices which are always preferred by crystallizable methylene sequences. This allows regioregular P3ATs to reach high degrees of crystalline order and perfection. In the case of regiorandom systems, the overall arrangement of main chains and side chains on the mesoscale is similar, but the main chains cannot crystallize due to the randomness of the distances between side chains along the main chain. Thus, the alkyl groups in the side chains can only crystallize if they are long and flexible enough similar to the situation discussed for other comblike polymers.[43] In this sense, regioregular P3ATs are more an exception as an archetype example for crystallizable side-chain polymers containing long alkyl groups since main chains and side chains do fit to the same lattice. This favors crystallization and allows the systems to exist in highly ordered states. Regiorandom P3ATs, however, are absolutely in line with common trends followed by many other comblike polymers thinking about the mesostructure, the general arrangement of main chains and side chains, and common features in their dynamics.

V. Conclusions and Outlook

Summarizing the results reported in this paper, one can conclude that regiorandom poly(3-alkylthiophenes) show typical features, which have been reported in the recent years for other side-chain polymers with long alkyl groups in the side chain. All investigated samples show in the amorphous state a prepeak at intermediate scattering vectors 0.255 $\leq q \leq$ 0.39 Å^{-1} corresponding to equivalent Bragg spacings in the range 16 $\leq d_{nps} \leq$ 24.5 Å. The d_{nps} value increases systematically with increasing side-chain length in accordance with the idea that the alkyl groups of different monomeric units tend to aggregate in the melt to form small alkyl nanodomains. Apart from the conventional α relaxation at high temperatures, which shifts with increasing C systematically to lower relaxation temperatures, an additional relaxation process within the alkyl nanodomains has been observed for all members with $6 \leq C \leq 12$ corresponding to the α_{PE} process, which is also seen for other series of side-chain

polymers with similar microstructure like atactic poly(*n*-alkyl methacrylates). This supports nanophase separation of main chains and alkyl groups in amorphous P3ATs. While regiorandom poly(3-alkylthiophenes) with $C = 4-8$ alkyl carbons per side chain are seemingly noncrystallizable, small crystalline fractions are observed for poly(3-decylthiophene) and poly(3-dodecylthiophene) ($C = 10, 12$). Interestingly, three distinct melting peaks between −5 and 25 °C seem to appear in regiorandom poly(3-dodecylthiophene) depending on the crystallization conditions. Speculatively, this indicates the occurrence of different polymorphs in the semicrystalline alkyl nanodoamins. An open point requiring further investigations is a better understanding of the crystalline state of P3DT and P3DDT. In particular, it is important to demonstrate finally that side-chain crystallization leads to different polymorphic states. This picture is supported by various experimental hints from calorimetry and X-ray scattering. For a final proof one can think about either more sensitive experimental methods, which can detect the crystalline packing in systems containing ≤10% crystalline CH_2 units, or experiments on regiorandom P3ATs with longer side chains ($C > 12$) and higher degree of crystallinity. An answer to the question whether or not different crystalline forms can grow in regiorandom P3DDT might be important from two different perspectives. First, it may contribute to a better understanding of structural details of regioregular poly(3-alkylthiophenes) where different crystalline forms may also exist.[36,37] Second, it is interesting in the light of the recent discussion about early stages of crystallization in bulk polyethylene[57−59] since conventionally unstable states may appear in equilibrium in small alkyl nanodomains. Further experimental as well as theoretical work should contribute to a better understanding of structural and thermodynamic aspects of amorphous side-chain polymers containing long methylene sequences. This would have high potential impact for future applications since various systems with similar microstructure are already used in different fields without clear knowledge about existing structure−property relationships.

Acknowledgment. The authors thank Ch. Eisenschmidt for assistance with the WAXS measurements, J. Lange and C. Schicktanz for IR and Raman spectroscopy experiments, and Th. Thurn-Albrecht and K. Schröter for helpful discussions. Financial support from the state Sachsen-Anhalt and the Deutsche Forschungsgemeinschaft (SFB 418) is gratefully acknowledged.

References and Notes

(1) Laschewsky, A.; Ringsdorf, H.; Schmidt, G.; Schneider, J. *J. Am. Chem. Soc.* **1987**, *109*, 788–796.
(2) Muthukumar, M.; Ober, C. K.; Thomas, E. L. *Science* **1997**, *277*, 1225–1232.
(3) Tschirske, C. *J. Mater. Chem.* **1998**, *8*, 1485–1508.
(4) Ikkala, O.; ten Brinke, G. *Science* **2002**, *295*, 2407–2409.
(5) Wegner, G. *Macromol. Phys. Chem.* **2003**, *204*, 347–357.
(6) Cowie, J. M. G.; Haq, Z.; McEwen, I. J.; Velickovic, J. *Polymer* **1981**, *22*, 327–332.
(7) Mena-Osteritz, K. E.; Meyer, A.; Langeveld-Voss, B. M. W.; Janssen, R. A. J.; Meijer, E. W.; Bäurele, P. *Angew. Chem., Int. Ed.* **2000**, *39*, 2679–2684.
(8) Beiner, M. *Macromol. Rapid Commun.* **2001**, *22*, 869–895.
(9) Stepanyan, R.; Subbotin, A.; Knaapila, M.; Ikkala, O.; ten Brinke, G. *Macromolecules* **2003**, *36*, 3658–3763.
(10) Beiner, M.; Huth, H. *Nat. Mater.* **2003**, *2*, 595–599.
(11) Arrighi, V.; Triolo, A.; McEwen, I. J.; Homes, P.; Triolo, R.; Amentisch, H. *Macromolecules* **2001**, *33*, 4989–4991.
(12) Chen, W.; Wunderlich, B. *Macromol. Chem. Phys.* **1999**, *200*, 283–311.
(13) Beiner, M.; Schröter, K.; Hempel, E.; Reissig, S.; Donth, E. *Macromolecules* **1999**, *32*, 6278–6282.
(14) Arbe, A.; Genix, A. C.; Colmenero, J.; Richter, D.; Fouquet, P. *Soft Matter* **2008**, *4*, 1792–1795.
(15) The prepeak as such could also appear in a disordered system with strong concentration fluctuations.[16−18] The existence of higher orders to the prepeak is a final proof for nanophase separation while the absence of higher orders is no criterion for mixing. Thermodynamically, a phase is defined as subsystem, which has uniform chemical composition and physical properties. "In other words, a phase consists of a homogeneous, macroscopic volume of matter, separated by well-defined surfaces of negligible influence on the phase properties.[19] Domains in a sample that differ in chemical composition or in physical state are considered to be different phases."[20] According to the classification by Wunderlich[20,21] "nanophases" are characterized by a certain influence of the surfaces on the properties. The appearance of a size-dependent but main-chain-independent dynamics within small alkyl nanodomains (α_{PE}) indicates their independence from the environment.
(16) de Gennes, P. G. *Scaling Concepts in Polymer Physics*, 4th ed.; Cornell University Press: Ithaca, NY, 1993.
(17) Ruokolainen, J.; Torkkeli, M.; Serimaa, R.; Komanschek, B. E.; Ikkala, O.; ten Brinke, G. *Phys. Rev. E* **1996**, *54*, 6646–6649.
(18) Strobl, G. *The Physics of Polymers*; Springer: Berlin, 1997.
(19) Gibbs, J. W. *Am. J. Sci.* **1878**, *16*, 441–458.
(20) Wunderlich, B. *Thermochim. Acta* **2003**, *403*, 1–13.
(21) Wunderlich, B. *Int. J. Thermophys.* **2007**, *29*, 958–967.
(22) Ngai, K. L.; Beiner, M. *Macromolecules* **2004**, *37*, 8123–8127.
(23) Hiller, S.; Pascui, O.; Budde, H.; Kabisch, O.; Reichert, D.; Beiner, M. *New J. Phys.* **2004**, *6*, 10.
(24) Gaborieau, M.; Graf, R.; Spiess, H. W. *Macromol. Chem. Phys.* **2008**, *209*, 2078−2086.
(25) Wind, M.; Graf, R.; Renker, S.; Spiess, H. W.; Steffen, W. *J. Chem. Phys.* **2005**, *122*, 014906.
(26) McCreight, K. W.; Ge, J. J.; Guo, M.; Hann, I.; Li, F.; Shen, Z.; Jin, X.; Harris, F. W. *J. Polym. Sci., Polym. Phys. Ed.* **1999**, *37*, 1633–1646.
(27) McCullough, R. D. *Adv. Mater.* **1998**, *10*, 93–116.
(28) Yazawa, K.; Inowe, Y.; Yamamoto, T.; Asakawa, N. *Phys. Rev. B* **2006**, *74*, 0942041−094204112.
(29) Prosa, T. J.; Winokur, M. J.; McCullough, R. D. *Macromolecules* **1996**, *29*, 3654–3656.
(30) Reynolds, J. R.; Reddinger, J. L. *Adv. Polym. Sci.* **1999**, *145*, 96–104.
(31) Inganäs, O.; Salaneck, W. R.; Österholm, H.; Laakso, J. *Synth. Met.* **1988**, *22*, 395–406.
(32) Rughoopth, S. D.; Hotta, S.; Hegger, A. J.; Wudl, F. *J. Polym. Sci., Polym. Phys. Ed.* **1987**, *25*, 1071–1078.
(33) Kline, R. J.; Delongchamp, D. M.; Fisher, D. A.; Lin, E. K.; Richter, L. J.; Chabinyc, M. L.; Toney, M. F.; Heeney, M.; McCulloch, I. *Macromolecules* **2007**, *40*, 7960–7965.
(34) McCullough, R. D.; Lowe, R. D.; Jayaraman, M.; Anderson, D. L. *J. Org. Chem.* **1993**, *58*, 904–912.
(35) McCullough, R. D.; Tristram-Nagle, S.; Williams, S. P.; Lowe, R. D.; Jayaraman, M. *J. Am. Chem. Soc.* **1993**, *115*, 4910–4911.
(36) Park, K. C.; Levon, K. *Macromolecules* **1997**, *30*, 3175–3183.
(37) Malik, S.; Nandi, A. K. *J. Polym. Sci., Polym. Phys. Ed.* **2002**, *40*, 2073–2085.
(38) Causin, V.; Marega, C.; Marigo, A.; Valentini, L.; Kenny, J. M. *Macromolecules* **2005**, *38*, 409–415.
(39) Hugger, S.; Thomann, R.; Heinzel, T.; Thurn-Albrecht, T. *Colloid Polym. Sci.* **2004**, *282*, 932–938.
(40) Winokur, M. J. In *Handbook of Conducting Polymers*, 2nd ed.; Skotheim, T. A., Elsenbaumer, R. L., Reynolds, J. R., Eds.; Marcel Dekker: New York, 1998; Chapter 25, pp 707−726.
(41) Schopf, G.; Kossmehl, G. *Adv. Polym. Sci.* **1997**, *129*, 36–50.
(42) Chen, T.; Wu, X.; Rieke, R. D. *J. Am. Chem. Soc.* **1995**, *117*, 233–244.
(43) Hempel, E.; Budde, H.; Höring, S.; Beiner, M. *J. Non-Cryst. Solids* **2006**, *352*, 5013–5020.
(44) The coherence length d_S has been estimated based on the Scherrer equation $d_S = K\lambda/(B \cos \theta)$ with $K = 0.9$ being the Scherrer constant, $\lambda = 1.54$ Å the wavelength of Cu Kα radiation, and B the full with at half-maximum in radians. Instrumental effects are neglected, and baseline contributions have been subtracted before determining B.
(45) Hempel, E.; Budde, H.; Höring, S.; Beiner, M. *Lect. Notes Phys.* **2007**, *714*, 201–228.
(46) Heijboer, J. In *Physics of Non-Crystalline Solids*; Prins, J. A., Ed.; North-Holland: Amsterdam, 1965; p 231.
(47) Johari, G. P.; Goldstein, M. *J. Chem. Phys.* **1970**, *53*, 2372–2388.
(48) Höhne, G. W. H. *Polymer* **2002**, *43*, 4689–4698.
(49) Shi, H.; Zhao, Y.; Jiang, S.; Xin, J. H.; Rottstegge, J.; Xu, D.; Wang, D. *Polymer* **2007**, *48*, 2762–2767.
(50) Shi, H.; Zhao, Y.; Zhang, X.; Jiang, S.; Wang, D.; Han, C. C.; Xu, D. *Macromolecules* **2004**, *37*, 9933–9940.
(51) Mierzwa, M.; Floudas, G.; Stepanek, P.; Wegner, G. *Phys. Rev. B* **2000**, *62*, 14012–14019.

(52) Broadhurst, M. G. *J. Res. Natl. Bur. Stand.* **1962**, *66A*, 241–249.
(53) Zheng, W. Y.; Levon, K.; Laakso, J.; Österholm, J. E. *Macromolecules* **1994**, *27*, 7754–7768.
(54) Zerbi, G.; Magni, R.; Gussoni, M.; Moritz, K. H.; Bigotto, A.; Dirlikov, S. *J. Chem. Phys.* **1981**, *75*, 3175–3194.
(55) Tashiro, S.; Sasaki, S.; Kobayashi, M. *Macromolecules* **1996**, *29*, 7460–7469.
(56) Sirota, E. B.; Herold, A. B. *Science* **1999**, *283*, 529–532.
(57) Strobl, G. *Eur. Phys. J. E* **2000**, *3*, 165–183. Strobl, G. *Prog. Polym. Sci.* **2006**, *31*, 398–442.
(58) Sirota, E. B. *Macromolecules* **2007**, *40*, 1043–1048.
(59) Beiner, M. *J. Polym. Sci., Polym. Phys. Ed.* **2008**, *46*, 1556–1561.

MA801633M